

Efficient and Scalable Estimation of Distributional Treatment Effects with Multi-Task Neural Networks

Tomu Hirata*, Undral Byambadalai†, Tatsushi Oka‡, Shota Yasui§, Shingo Uto¶

July 11, 2025

Abstract

We propose a novel multi-task neural network approach for estimating distributional treatment effects (DTE) in randomized experiments. While DTE provides more granular insights into the experiment outcomes over conventional methods focusing on the Average Treatment Effect (ATE), estimating it with regression adjustment methods presents significant challenges. Specifically, precision in the distribution tails suffers due to data imbalance, and computational inefficiencies arise from the need to solve numerous regression problems, particularly in large-scale datasets commonly encountered in industry. To address these limitations, our method leverages multi-task neural networks to estimate conditional outcome distributions while incorporating monotonic shape constraints and multi-threshold label learning to enhance accuracy. To demonstrate the practical effectiveness of our proposed method, we apply our method to both simulated and real-world datasets, including a randomized field experiment aimed at reducing water consumption in the US and a large-scale A/B test from a leading streaming platform in Japan.¹ The experimental results consistently demonstrate superior performance across various datasets, establishing our method as a robust and practical solution for modern causal inference applications requiring a detailed understanding of treatment effect heterogeneity.

Keywords: randomized experiment, distributional treatment effect, multi-task learning, neural network, shape constraints

*Databricks Japan, Inc, Tokyo, Japan (tomu.hirata@databricks.com)

†CyberAgent, Inc, Tokyo, Japan (undral.byambadalai@cyberagent.co.jp)

‡Department of Economics, Keio University, Tokyo, Japan (tatsushi.oka@keio.jp)

§CyberAgent, Inc, Tokyo, Japan (yasui.shota@cyberagent.co.jp)

¶AbemaTV, Tokyo, Japan (uto.shingo@abema.tv)

¹The proposed algorithm is available in the Python library `dte-adj` (<https://pypi.org/project/dte-adj/>)

1 Introduction

Randomized experiments, also known as A/B tests, have served as a cornerstone for understanding intervention effects and shaping policy decisions since Fisher’s seminal work [27]. The framework of causal inference through randomized experiments has become foundational across diverse scientific disciplines [52, 36, 51] and has been widely adopted by technology companies as a standard practice in their decision-making processes [56, 61, 39].

While the Average Treatment Effect (ATE) is the conventional measure in randomized experiments, it is subject to two significant limitations: imprecise estimates with high variance relative to their magnitudes [41], and incomplete characterization of intervention impacts across the outcome distribution. Although numerous studies have proposed methods for capturing distributional impacts of treatments [1, 26, 50, 3, 28, 40, 17], addressing both estimation precision and distributional characterization remains a challenge.

In this paper, we propose a novel approach to estimating Distributional Treatment Effects (DTE) using multi-task neural networks (NN). The DTE captures comprehensive treatment effects by measuring changes across the outcome distribution induced by treatments. While DTE estimation can be performed by directly comparing empirical outcome distributions between treatment and control groups, this approach often overlooks valuable pre-treatment auxiliary information commonly available in randomized experiments. Our method extends existing regression-adjustment techniques that leverage pre-treatment covariates for ATE estimation, an approach widely adopted in industry to enhance experimental sensitivity [23, 62]. By incorporating regression-adjustment methods within a neural network architecture for distributional regression, we develop a more powerful framework for DTE estimation.

Our proposed method enhances estimation precision, particularly in the distribution tails, through a multi-task neural network architecture with shape restrictions that jointly learns from multiple parts of the outcome distribution. By estimating distributional features simultaneously rather than solving separate regression problems, our method achieves significant computational efficiency. These methodological advances prove particularly valuable for analyzing large-scale datasets commonly encountered in industrial applications, as demonstrated in a US water conservation experiment and a large-scale A/B test on a Japanese streaming platform.

Our primary contributions are summarized as follows:

- We propose multi-task neural networks for estimating conditional outcome distributions, substantially improving computational efficiency. For illustration, see Figure 1.
- We improve the estimation precision of distributional treatment effects by incorporating shape constraints into the neural network.
- We validate the efficacy of our proposed methodology through extensive simulation studies and empirical analyses of two real-world datasets.

The rest of this paper is structured as follows. Section 2 describes related research. We explain the problem setup in Section 3 and the proposed methodology in Section 4. Section 5 presents simulation studies and two real-world applications. We conclude the paper in Section 6. The Appendix in the paper includes additional details and results.

2 Related Work

Distributional Treatment Effect: Although the ATE remains a standard metric in treatment evaluation, the distributional characterization of treatment effects provides more comprehensive insights into treatment

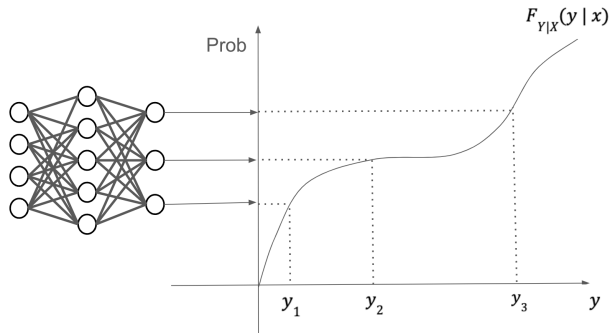


Figure 1: Illustration: Multi-Task neural network estimating the conditional distribution function $F_{Y|X}(\cdot|x)$.

heterogeneity. This has motivated extensive research on both Quantile Treatment Effects (QTE) and Distributional Treatment Effects (DTE) [1, 17, 3, 9, 15, 16, 38, 30, 10, 63]. Unlike QTE which requires continuous outcome distributions, DTE can be applied to both discrete and continuous outcomes.

Regression Adjustment: When estimating the treatment effect of RCT, the sensitivity of the estimation is critical. For example, failure to detect an effect due to a large variance leads to potential revenue loss in industry. Regression adjustment is a method that utilizes pre-treatment covariates to estimate the treatment effect more precisely. Various researches have explored the usage of regression adjustment to gain precise estimation for the ATE including [29, 6, 43, 49, 58, 35, 48, 64]. Despite the challenges in learning a correct relationship between pre-treatment covariates and outcome variables, it has been proved that the regression-adjusted estimation is unbiased, consistent, and practically useful. Recent studies have extended regression adjustment beyond ATE to distributional treatment effects, establishing theoretical foundations for its application [37, 46, 8, 7]. Building on this line of work, we enhance regression adjustment for distributional treatment effects by improving the underlying algorithm and integrating recent advancements in deep learning.

Multi-Task Learning: Multi-task learning enables a single model to learn multiple related tasks simultaneously, leveraging shared representations to enhance performance [11, 68, 53, 21]. This joint learning strategy improves generalization and mitigates overfitting [69]. The framework proves particularly valuable in multi-label classification, where outputs can belong to multiple categories simultaneously [57, 67]. By treating each label prediction as a distinct yet related task, multi-task learning effectively captures label dependencies [66, 22, 54] and leverages shared patterns within a unified framework [2]. The deep neural network approach has been studied to estimate distributional regression based on binary cross-entropy [42] and quantile regression [55, 59]. Our approach reformulates distributional regression as a multi-label classification task, utilizing multi-task learning to share representations across the distribution.

Shape Restriction: Shape restriction on statistical models has a long history in statistics and econometrics, and there is a broad range of research about various shape restrictions such as concavity or monotonicity for parametric or semiparametric statistical models [4, 33, 45, 34, 18, 24]. These shape restrictions are used for stabilizing the semiparametric models or increasing the efficiency of the estimation. They work particularly well if simple estimation is difficult due to a small sample size. Recent studies explored the shape restriction on machine learning (ML) models with higher dimensions of covariates [32, 65, 31, 20], ensuring the monotonic relationship between input variables and outputs of neural networks. Wu et al. [60] incorporated a cumsum function to ensure the monotonicity of individualized treatment effects (ITEs) estimation across different quantiles. In this study, we introduce a monotonic constraint on the output of neural networks to enhance the stability and precision of unconditional treatment effects.

3 Problem Setup

3.1 Setup and Notation

We consider a randomized experiment with K treatment arms, where each unit is assigned to treatment w with probability $\pi_w := P(W = w)$ such that $\sum_{w \in \mathcal{W}} \pi_w = 1$. The observed data consist of n independent samples $\{(X_i, W_i, Y_i)\}_{i=1}^n$ from (X, W, Y) , where $X \in \mathcal{X} \subseteq \mathbb{R}^{d_x}$ is a vector of pre-treatment covariates, $W \in \mathcal{W} := \{1, \dots, K\}$ is the treatment assignment, and $Y \in \mathcal{Y} \subseteq \mathbb{R}$ is the observed outcome. Under the potential outcomes framework [51, 52, 36], each unit has potential outcomes $Y(1), \dots, Y(K)$, but only the outcome corresponding to the assigned treatment is observed, denoted as $Y = Y(W)$. Each treatment group contains n_w observations, satisfying $\sum_{w \in \mathcal{W}} n_w = n$.

Throughout the paper, we maintain the following assumptions:

Assumption 1. $Y(1), \dots, Y(K), X \perp\!\!\!\perp W$.

Assumption 2. $0 < \pi_w < 1, \quad \forall w \in \mathcal{W}$.

Assumption 1 ensures treatment assignment is independent of potential outcomes and pre-treatment covariates, while Assumption 2 guarantees non-zero assignment probabilities. These assumptions are valid under randomized experiments.

We define the cumulative distribution functions (CDFs) of potential outcomes as:

$$F_{Y(w)}(y) := \Pr(Y(w) \leq y),$$

for $y \in \mathcal{Y} \subseteq \mathbb{R}$ and $w \in \mathcal{W}$. While potential outcomes are unobservable, the potential outcome distribution $F_{Y(w)}(y)$ becomes identifiable when Assumptions 1 and 2 are satisfied, as it equals the observed outcome distribution $F_{Y|W}(y|w) := \Pr(Y \leq y | W = w)$ for each treatment w . In practice, we usually have a set of scalar-valued locations $\tilde{\mathcal{Y}} \subseteq \mathcal{Y}$ for which cumulative distribution functions are estimated and the following set of parameters are computed together:

$$\mathcal{F}_{Y(w)} := \{F_{Y(w)}(y) | y \in \tilde{\mathcal{Y}}\}.$$

This collection of CDFs provides a distributional characterization of the treatment effect across the outcome distribution.

3.2 Distributional Treatment Effect

We formally define the *Distributional Treatment Effect* (DTE) between treatments $w, w' \in \mathcal{W}$ as

$$\Delta_{w,w'}^{DTE}(y) := F_{Y(w)}(y) - F_{Y(w')}(y),$$

for $y \in \mathcal{Y}$. The DTE measures the difference between CDFs of the potential outcomes under the two treatments.

While our primary focus is the DTE, our framework extends to any parameters obtained through transformations of CDFs. An important example is the *Probability Treatment Effect* (PTE) between treatments $w, w' \in \mathcal{W}$, defined as

$$\Delta_{w,w'}^{PTE}(y_j) := f_{Y(w)}(y_j) - f_{Y(w')}(y_j),$$

where

$$\begin{aligned} f_{Y(w)}(y_j) &:= \Pr(y_{j-1} < Y(w) \leq y_j) \\ &= F_{Y(w)}(y_j) - F_{Y(w)}(y_{j-1}), \end{aligned}$$

for $y_j \in \mathcal{Y}$. Each quantity $f_{Y(w)}(y_j)$, which we refer to as the *interval probability*, represents the difference between consecutive CDF values at y_j and y_{j-1} . The PTE measures the differences in these interval probabilities between treatments.

4 Estimation Methods

In this section, we describe our proposed method and its advantages. As a prerequisite, the existing algorithm is explained below.

4.1 Single-Task Regression Adjustment Algorithm and its Limitations

We describe the existing regression-adjusted estimation procedure for distribution functions, which is outlined in Algorithm 1. The procedure begins with estimating the conditional distribution function of $Y(w)$ given X , defined as

$$\gamma_y^{(w)}(X) := \Pr(Y(w) \leq y | X),$$

and let $\hat{\gamma}_y^{(w)}(X)$ denote its estimator for each $y \in \mathcal{Y}$ and $w \in \mathcal{W}$. The estimation can be reformulated as a prediction problem by noting that $\gamma_y^{(w)}(X) = E[\mathbf{1}_{\{Y(w) \leq y\}} | X]$, wherein we predict binary outcomes $\mathbf{1}_{\{Y(w) \leq y\}}$ using pre-treatment covariates X through a supervised learning algorithm \mathcal{S} (e.g., linear regression, gradient boosting, random forests, single-task neural network). The estimation procedure relies on a sample-splitting method called cross-fitting, which, combined with the Neyman orthogonality, enables us to derive the asymptotic distribution of the regression-adjusted estimator under mild conditions [12].

Then, the regression-adjusted estimator of $F_{Y(w)}(y)$ is computed as follows:

$$\hat{F}_{Y(w)}(y) = \frac{1}{n_w} \sum_{i:W_i=w} (\mathbf{1}_{\{Y_i \leq y\}} - \hat{\gamma}_y^{(w)}(X_i)) + \frac{1}{n} \sum_{i=1}^n \hat{\gamma}_y^{(w)}(X_i). \quad (1)$$

This estimator modifies the empirical distribution function by subtracting the treatment group average of $\hat{\gamma}_y^{(w)}(\cdot)$ and adding its overall average. The resulting estimator is unbiased since the expected values of these adjustment terms cancel out.

Algorithm 1 Single-Task Regression-Adjustment Algorithm

Input: Data $\{(X_i, W_i, Y_i)\}_{i=1}^n$ split randomly into L roughly equal-sized folds ($L > 1$); a supervised learning algorithm \mathcal{S} .

- 1: **for** treatment group $w \in \mathcal{W}$ **do**
 - 2: **for** level $y \in \tilde{\mathcal{Y}}$ **do**
 - 3: **for** fold $\ell = 1$ to L **do**
 - 4: Train \mathcal{S} on data excluding fold ℓ ,
 - 5: using observations in treatment group w .
 - 6: Use \mathcal{S} to predict $\hat{\gamma}_y^{(w)}(X_i)$ for each X_i in fold ℓ .
 - 7: **end for**
 - 8: Compute $\hat{F}_{Y(w)}(y)$ according to equation (1).
 - 9: **end for**
 - 10: **end for**
-

Moreover, the following theorem holds for the adjusted estimator in equation (1) highlighting the efficiency gain through the regression adjustment compared with the empirical estimation defined by $\hat{\mathbf{F}}_{Y(w)}^{\text{empirical}}(y) :=$

$\sum_{i:W_i=w} \mathbf{1}_{\{Y_i \leq y\}}/n_w$. Consider the scenario where the true conditional distribution function, $\gamma_y^{(w)}(\cdot)$, is employed in (1), leading to the idealized form of the regression-adjusted estimator, denoted by $\tilde{\theta}_y^{(w)} := \tilde{F}_{Y(w)}(y)$. Let the vector version be denoted by $\tilde{\theta}_y := (\tilde{\theta}_y^{(1)}, \dots, \tilde{\theta}_y^{(K)})^\top$.

Theorem 1. *Suppose that $n_w/n = \pi_w + o(1)$ as $n \rightarrow \infty$ for every $w \in W$. Then, the following inequalities hold:*

(a) for any $w \in W$ and $y \in \mathcal{Y}$,

$$\text{Var}(\hat{\mathbf{F}}_{Y(w)}^{\text{empirical}}(y)) \geq \text{Var}(\tilde{\mathbf{F}}_{Y(w)}(y)) + o(n^{-1}),$$

where the equality holds only if $F_{Y(w)|X}(y) = F_{Y(w)}(y)$,

(b) for any $y \in \mathcal{Y}$,

$$\text{Var}(\hat{\theta}_y^{\text{empirical}}) \succeq \text{Var}(\tilde{\theta}_y) + o(n^{-1}),$$

where \succeq denotes the positive semi-definiteness. When $\text{Var}(F_{Y(w)}(y|X) - r \cdot F_{Y(w')}(y|X)) > 0$ for any distinct $w, w' \in W$ and $r \in \mathbb{R}$, the positive definite result holds.

Theorem 1(a) states the variance reduction accomplished by applying regression adjustment to distribution functions. Additionally, Theorem 1(b) elaborates on this variance reduction as a vector of regression-adjusted estimators, indicating the efficiency gain of the adjusted estimator for the DTE as a special case.

Despite effectively leveraging semiparametric models in conjunction with cross-fitting [12, 13], the algorithm has several limitations. First, the algorithm has a high computational cost due to the need for iterations of single-target regression problems. The computational complexity of the algorithm is $O(M \cdot D \cdot L \cdot P)$, where M indicates the number of locations, D indicates the number of treatment levels, L indicates the number of folds, and $P := \text{Cost}(\mathcal{S}(1))$ indicates the computational cost of one iteration of the supervised statistical model training \mathcal{S} for one target variable. When the number of locations is large, this algorithm takes a long time to compute the adjusted distributional parameters due to many iterations of ML model training. Moreover, estimating the conditional distribution function is particularly challenging in the distribution tails due to label imbalance. For instance, when estimating the cumulative probability at the 90th percentile, 90% of the training data satisfies $\mathbf{1}_{\{Y \leq y\}} = 1$, leading to difficulties in handling the imbalance. A similar issue arises at lower percentiles, where the majority of labels take the opposite value.

4.2 Multi-Task Regression Adjustment Algorithm

In this study, we reformulate the distribution regression into a multi-label classification task and propose a novel algorithm to estimate the regression-adjusted distribution function by leveraging a multi-task statistical

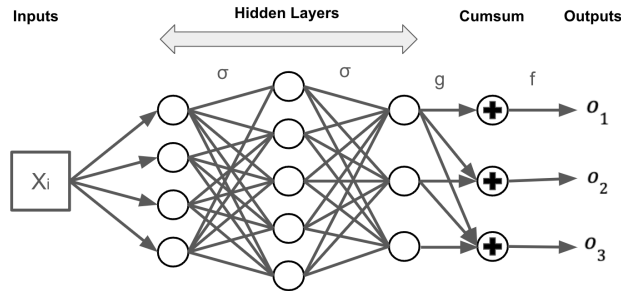


Figure 2: Illustration of the architecture of the proposed neural network model. The model accumulates the output of the hidden layers to have the monotonicity of the final outputs.

model for estimating conditional distribution function $\hat{\gamma}_y^{(w)}(X)$ for all $y \in \tilde{\mathcal{Y}}$ simultaneously. The procedure estimates a set of conditional distribution functions, defined as

$$\Gamma^{(w)} := \{\gamma_y^{(w)}(\cdot) \mid y \in \tilde{\mathcal{Y}}\}.$$

and let $\hat{\Gamma}^{(w)}$ be its estimator for each $w \in \mathcal{W}$ instead of estimating $\hat{\gamma}_y^{(w)}(X)$ for each $y \in \tilde{\mathcal{Y}}$ individually.

The proposed method aims to overcome the high computational cost of the existing algorithm based on the following Assumption 3, where $\mathcal{S}(M)$ indicates the multi-task supervised learning algorithm with the number of target variables equal to M . This assumption posits that the computational cost of training the machine learning model increases at a sublinear rate for the size of the target variables.

Assumption 3.

$$\tilde{P} := \text{Cost}(\mathcal{S}(M)) < O(P \cdot M).$$

If a single multi-task ML model is trained for all locations together and the computation cost for the single model is \tilde{P} , the total computation cost of the entire estimation process is $O(D \cdot L \cdot \tilde{P})$, which is lower than the existing algorithm $O(M \cdot D \cdot L \cdot P)$ when Assumption 3 is met. Note that Assumption 3 is not strong as many statistical models that can estimate multiple target variables together satisfy the assumption, including Linear Regression, Lasso, and Neural Networks. Appendix G presents the theoretical analysis of the sub-linear assumption for linear regression and the empirical results of computational complexity across multiple neural network models. However, some algorithms, such as gradient-boosting trees or random forests, do not fulfill this condition since these algorithms need one model per target and usually the One vs Rest strategy is adopted for multi-output learning. The proposed algorithm for estimating the regression-adjusted distribution function with a multi-task ML model is available in Algorithm 2 where $\hat{\mathcal{F}}_{Y^{(w)}} := \{\hat{F}_{Y^{(w)}}(y) \mid y \in \tilde{\mathcal{Y}}\}$.

Algorithm 2 Multi Task Regression-Adjustment Algorithm

Input: Data $\{(X_i, W_i, Y_i)\}_{i=1}^n$ split randomly into L roughly equal-sized folds ($L > 1$); a multi-task supervised learning algorithm $\mathcal{S}(M)$.

- 1: **for** treatment group $w \in \mathcal{W}$ **do**
 - 2: **for** fold $\ell = 1$ to L **do**
 - 3: Train $\mathcal{S}(M)$ on data excluding fold ℓ ,
 - 4: using observations in treatment group w .
 - 5: Use $\mathcal{S}(M)$ to predict $\hat{\Gamma}^{(w)}$ for observations in fold ℓ .
 - 6: **end for**
 - 7: Compute $\hat{\mathcal{F}}_{Y^{(w)}}$ according to equation (1).
 - 8: **end for**
-

Beyond computational efficiency, the multi-task model can learn richer representations compared to a single model trained for a single location. By simultaneously estimating multiple locations, the multi-task approach helps mitigate the label imbalance issue discussed in the previous section. Since the underlying relationship between covariates and the outcome remains consistent across locations, sharing representations through multi-task learning may improve estimation precision, as suggested in previous research [21].

Moreover, using a single multi-task ML model for estimating cumulative probability for each $y \in \tilde{\mathcal{Y}}$ enables us to enforce a monotonicity constraint across estimated probabilities in multiple locations. Specifically, for all $w \in \mathcal{W}$, the true conditional distribution function satisfies the following:

$$\gamma_{y_s}^{(w)}(X) \geq \gamma_{y_t}^{(w)}(X), \quad \forall y_s, y_t \in \mathcal{Y} \text{ s.t. } y_s \geq y_t \text{ a.s.} \quad (2)$$

Since the true function satisfies the monotonicity property above, enforcing this constraint not only enhances interpretability [31, 65], but also has the potential to improve training efficiency, as suggested by previous research [18]. Specifically, for all $w \in \mathcal{W}$ and $X_i \in \mathcal{X}$, the estimated probabilities must satisfy

$$\hat{\gamma}_{y_s}^{(w)}(X_i) \geq \hat{\gamma}_{y_t}^{(w)}(X_i), \quad \forall y_s, y_t \in \tilde{\mathcal{Y}} \text{ s.t. } y_s \geq y_t. \quad (3)$$

This monotonicity constraint, which may not be ensured when training separate single-task ML models for each target variable, can be enforced through a multi-task ML model. In this study, the DTE regression adjustment model is implemented based on a fully connected neural network. The architecture is illustrated in Figure 2. In this figure, $\sigma : \mathcal{X} \rightarrow \mathbb{R}$ is an activation function (e.g., ReLU or Sigmoid) used within the hidden layers, $g : \mathbb{R} \rightarrow [0, \infty)$ is a monotonic non-negative function for the last hidden layer, and $f : [0, \infty) \rightarrow [0, 1]$ represents a monotonic map to compute the output probabilities.

In our proposed model, the monotonic constraint of the outputs is accomplished by the combination of g and f . Let H denote the number of hidden layers, h_j^k be the j th element of the hidden layer $k \in \{1, 2, \dots, H\}$, and $o_j := \hat{\gamma}_{y_j}^{(w)}(X)$ be the j th element of the final output. Also, suppose $\tilde{\mathcal{Y}}$ is sorted before training the model. The layers up to the final hidden layer are standard fully-connected neural network layers. In the final hidden layer H , a vector of non-negative values is obtained by applying g to its output. Then, a vector of non-negative values $\tilde{h}^H = \{\tilde{h}_1^H, \tilde{h}_2^H, \dots, \tilde{h}_M^H\}$ is computed where each component \tilde{h}_j^H is obtained by accumulating the non-negative components up to that point from the previous layer as

$$\tilde{h}_j^H = \sum_{m=1}^j g(h_m^H), \quad \forall j \in \{1, 2, \dots, M\}.$$

Then, by construction, its elements satisfy the monotonicity property:

$$\tilde{h}_s^H \geq \tilde{h}_t^H, \quad \forall s, t \in \{1, 2, \dots, M\} \text{ s.t. } s \geq t.$$

Finally, the final output is obtained by applying f function to each component in the last hidden layer as $o_j = f(\tilde{h}_j^H)$ for $j \in \{1, \dots, M\}$, and satisfies the monotonicity property given in (3) by applying the monotonic function f to the monotonically increasing vector.

5 Empirical Results

In this section, we evaluate our proposed multi-task regression-adjusted estimators against other methods in three distinct settings: simulation studies, a water conservation experiment, and a content promotion A/B test at a Japanese video streaming platform.

5.1 Simulation

We conduct a Monte Carlo simulation study to assess the finite-sample performance of our adjusted estimators. Specifically, we evaluate the effectiveness of the proposed multi-task neural networks model adjustment in variance reduction, comparing it with the empirical distribution function, linear regression adjustment and the single-task NN model adjustment. The details of the data generation process (DGP) are provided in Appendix D.1.

For each simulation iteration, we generate a sample of size $n = 1000$ following the specified DGP and compute the distributional treatment effects (DTE) at quantiles $\{0.05, 0.10, \dots, 0.95\}$. This process is repeated $S = 500$ times. To establish a ground truth for evaluating estimation efficiency, we separately generate 10^5 samples from the same DGP and compute the corresponding DTE, which is used to calculate bias and mean squared error (MSE). The details of the multi-task NN model are described in Appendix D.2.

Figure 3 illustrates the reduction rate of pointwise MSE for each method compared to the empirical method across different locations, where higher values indicate greater precision. The results indicate that the multi-task NN adjustment method, both with and without the monotonic constraint, reduces pointwise MSE by 50–65%. This reduction is greater than that of the single-task NN adjustment and linear regression adjustment, which achieve reductions of 12–50%. Notably, at the tails of the distribution, such as $q = 0.05$ and $q = 0.95$, the reduction in MSE is particularly pronounced.

Since all estimators used in the experiment are unbiased, there is no substantial difference in bias values. Therefore, the observed differences in MSE are primarily attributable to variance reduction. These results indicate that multi-task learning significantly contributes to variance reduction. Moreover, since the monotonic multi-task NN adjustment method demonstrates the best performance, the monotonic restriction also contributes the variance reduction.

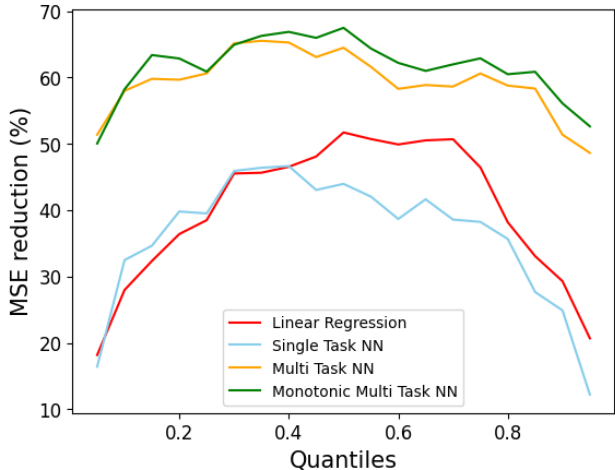


Figure 3: Pointwise MSE Reduction (%) relative to the empirical DTE in the Simulation Study. DTE is computed for each quantile $q \in \{0.05, 0.1, \dots, 0.95\}$.

To evaluate the efficiency gains achieved through multi-task learning, we measured the average execution time of the estimation over 500 repetitions for each method. As presented in Table 1, the average execution time of the multi-task NN adjustment is significantly lower than that of the single-task NN adjustment method.

By leveraging the multi-task learning, the computation time for adjusted DTE estimation is reduced by around 80% over the single-task NN adjustment under this simulation setting, highlighting the efficiency of the proposed approach.

We also validate whether the improvement in the precision of distribution function estimation can be attributed to the enhancement of model prediction performance. To investigate this, we compare the prediction performance of linear regression, the single-task NN model, the multi-task NN model, and the monotonic multi-task NN model on a binary classification problem. We use the same data and locations of the simulation study and aggregate the prediction performance across all locations.

The prediction performance of each model obtained from 2-fold cross-validation is presented in Table A5. As shown in the numerical results, the multi-task and the monotonic multi-task NN models outperform other models. This result suggests that multi-task learning contributes to prediction performance at each location. Additionally, although the contribution is smaller compared to multi-task learning, the monotonic restriction also improves prediction performance. This result suggests that the improvement in precision for distribution function estimation is primarily driven by the superior predictive capability of the proposed monotonic multi-task NN model.

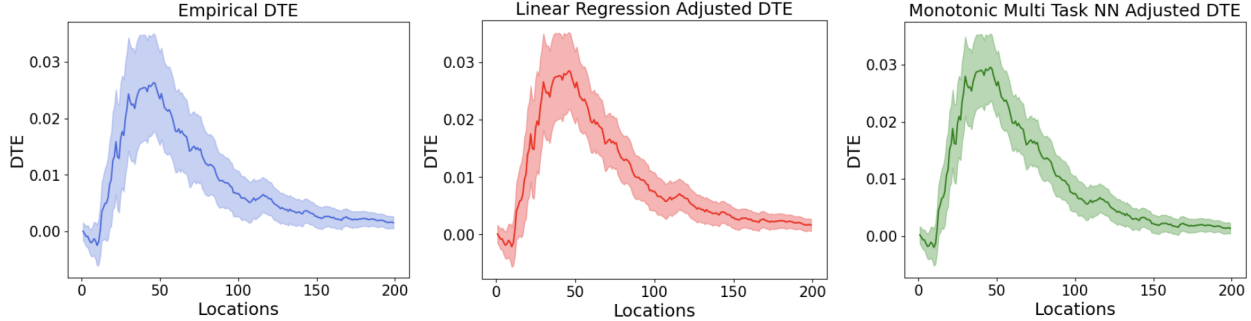


Figure 4: Distributional Treatment Effect (DTE) of a nudge (Strong Social Norm vs. Control) on water consumption (in thousands of gallons). The left figure shows the empirical DTE, the middle figure shows the linear adjusted DTE, and the right figure shows the monotonic multi-task NN adjusted DTE, computed for $y \in \{1, 2, \dots, 200\}$.

Method	(1) Simulation	(2) Nudge	(3) ABEMA
Linear Regression	0.187 (sd 0.115)	125	1,905
Single-Task NN	7.89 (sd 0.609)	1,888	8,249
Multi-Task NN	1.71 (sd 0.126)	124	2,087
Monotonic Multi-Task NN	1.61 (sd 0.132)	127	2,382

Table 1: Execution Times in seconds for Different Methods Across Datasets. Rows represent methods and columns represent experimental datasets.

5.2 Nudges to Reduce Water Consumption

In this section, we evaluate the performance of the proposed method using publicly available real randomized experiment data.

Specifically, we reanalyze data from a randomized experiment conducted by Ferraro and Price [25] in 2007, which examined the impact of norm-based messages, or “nudges,” on water consumption in Cobb County, Atlanta, Georgia. The experiment involved three distinct interventions designed to reduce water usage, each compared to a control group that received no nudge.

List et al. [44] re-estimated the ATE for the intervention labeled “strong social norm,” which incorporated both a prosocial appeal and social comparison, making it the most intensive intervention applied. Building on their analysis, we estimate the regression-adjusted DTE for this intervention relative to the control group, utilizing the same set of pre-treatment covariates, X , representing monthly water consumption during the year preceding the experiment. Consequently, the covariate space X has a dimensionality of $d_x = 12$. The outcome variable Y represents water consumption levels from June to September 2007, measured in thousands of gallons and treated as discretely distributed.

Figure 4 presents the DTE estimation results using the empirical cumulative distribution function (CDF), linear regression adjustment, single-task NN adjustment, and the proposed multi-task NN adjustments. We calculate and compare standard errors (SE) using a multiplier bootstrap with $B = 5,000$ repetitions for each method as explained in Appendix C. Regardless of the method used, the results show an increase in the number of users with a consumption level of around 10-50 in the treatment group, while the number of users with higher consumption levels has decreased.

In real-world data, the true effect cannot be observed, so we cannot calculate MSE as in the previous section. Instead, we examine whether SE has been reduced. To examine the reduction in SE, we calculated

the pointwise SE reduction relative to the empirical DTE for each location and presented it in Figure 5. The proposed method achieves a standard error reduction of 0–30%, outperforming both the linear regression adjustment and the single-task NN adjustment. The methods using multi-task learning show a smaller difference in SE than single-task learning for the location between 0 and 100. On the other hand, for locations greater than 100, SE is more significantly reduced with multi-task learning. Predictions in the range of 100 to 200 are more challenging, as more than 95% of records fall within the range of 0 to 100, as illustrated in Figure A1 of Appendix E.

The enhanced precision in this region suggests that learning labels jointly across all locations enables the model to better capture the underlying distribution and address the imbalanced data issue effectively. Though not significant, SE is reduced further around the tail of the distribution by the monotonic constraint.

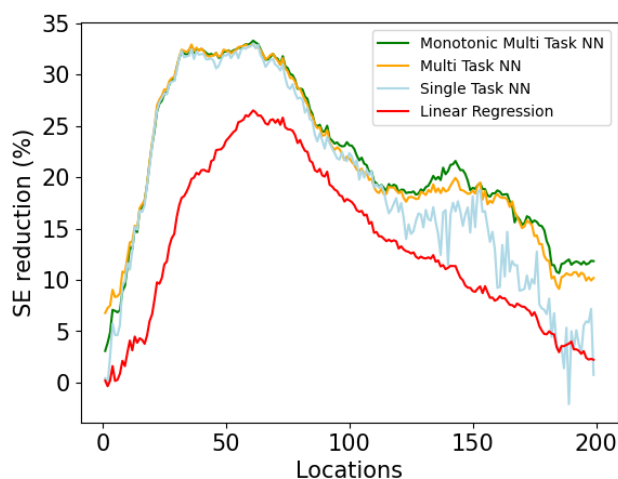


Figure 5: Pointwise SE reduction (%) relative to the empirical DTE of a nudge on water consumption.

5.3 ABEMA Content Promotion

Lastly, the proposed regression adjustment methods are applied to evaluate the result of an A/B test at ABEMA, a leading video streaming platform in Japan with over 30 million weekly active users. The A/B test was conducted to investigate the impact of top-of-screen content promotions in the ABEMA mobile application on viewer engagement over a four-week period. In the experiment, users were randomly assigned to one of two treatment groups: those exposed to content promotions and those exposed to advertisements. Figure 6 illustrates these two treatment conditions with screen captures.

The outcome variable in this experiment is the total viewing time (in minutes) for a selected series over the four-week experiment period. The pre-treatment covariates include age, gender, and various historical user activities recorded during the three weeks preceding the experiment. See Appendix F for experiment settings. For this analysis, we focus on a 46-minute comedy program. The experiment included a total of 4,311,905 users, which is a subset of total platform users.

The estimated ATE of the content promotion is 0.0145 (SE = 0.006, $p = 0.01$) minutes, corresponding to a 5.9% increase in the average viewing time. This result indicates that the promotion successfully increased users’ average viewing duration. However, an increase in average viewing time can arise from multiple scenarios, such as a rise in new users watching the content, a significant increase in users who watch for a short duration, or a growth in users who watch for a relatively long duration. The estimated average treatment effect does not provide particularly useful information in distinguishing between these scenarios.

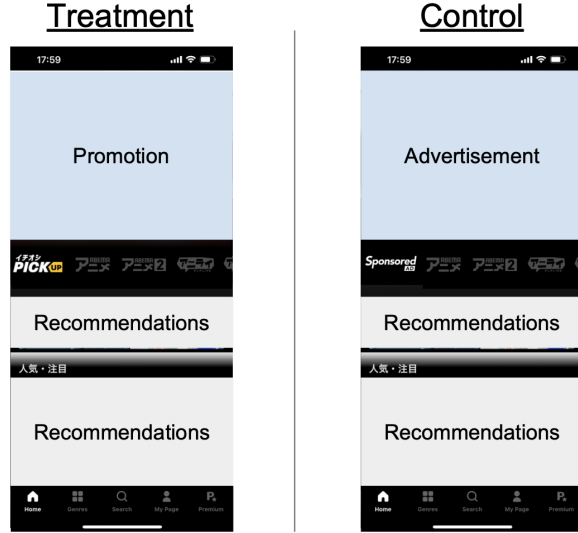


Figure 6: Top-of-Screen promotion in ABEMA application. Screen captures showing the two treatment conditions: content promotion (left) and advertisement (right).

To examine the heterogeneous effects, we estimate the DTE. Figure 7 presents the DTE estimation results using the empirical CDF, linear regression adjustment, and the proposed multi-task NN adjustments. Regardless of the method used, it is shown that there are fewer users in the treatment group at $y = 0$. This indicates that content promotion primarily encouraged users to start watching the series and reduced the number of users who did not engage with the content at all. Additionally, for $y > 0$, the number of users in the treatment group has increased, with a particularly larger increase among users who watched for a short duration. This suggests that while some users exposed to content promotion complete viewing, many others engage only briefly.

As illustrated in the SE reduction comparisons in Figure 8, all methods improve estimation precision relative to the empirical estimation. The SE reduction is relatively small at $y = 0$ but increases for $y > 0$, where the number of observations is lower. The proposed multi-task NN adjustment and monotonic multi-task NN adjustment achieve the highest SE reduction across most locations, reducing SE by 0–16%.

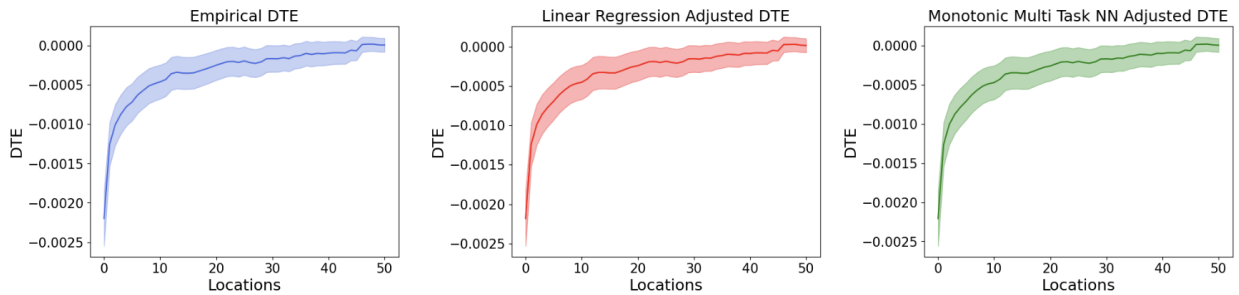


Figure 7: Distributional Treatment Effect (DTE) of the content promotion on ABEMA. The left figure shows the empirical DTE, the middle figure shows the linear adjusted DTE, and the right figure shows the monotonic multi-task NN adjusted DTE, computed for $y \in \{0, 1, 2, \dots, 50\}$.

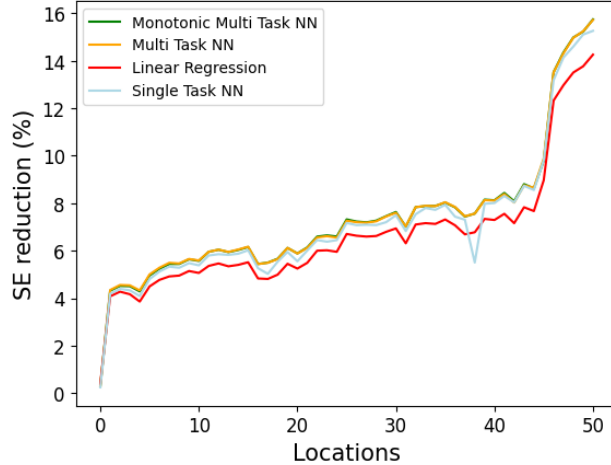


Figure 8: Pointwise SE reduction (%) relative to empirical DTE of content promotion on 46-minute program viewing time.

Finally, we compare computational times across methods using two real-world datasets in Table 1. Our multi-task neural network implementation demonstrates substantial computational advantages, yielding execution time reductions of 93% and 71% in the first and second experiments, respectively, compared to the single-task neural network implementation.

6 Conclusion

In this study, we introduce a novel multi-task neural network approach with monotonic shape constraints for efficiently estimating distributional treatment effects in randomized experiments. Our method reduces computational costs drastically by leveraging multi-task learning, while enhancing precision through the monotonic shape constraint and multi-label learning. Theoretical analysis establishes the efficiency gains of our approach, and empirical results confirm significant reductions in execution time alongside improved estimation precision.

The method’s computational advantages and shared representations are most pronounced when estimating cumulative distribution functions at multiple locations, though these benefits may be more modest for scenarios with fewer estimation points. Additionally, the computational efficiency gains depend on Assumption 3, and may vary under different model architectures such as boosting trees. Nevertheless, our approach represents a significant advancement in the estimation of distributional treatment effects, offering a scalable and practical solution for modern large-scale randomized experiments. The framework we establish opens new possibilities for efficient treatment effect analysis across diverse experimental settings.

References

- [1] Alberto Abadie. Bootstrap tests for distributional treatment effects in instrumental variable models. *Journal of the American Statistical Association*, 97:284–292, 2002.
- [2] Andreas Argyriou, Theodoros Evgeniou, and Massimiliano Pontil. Multi-task feature learning. *Advances in Neural Information Processing Systems*, 19:41–48, 2007.
- [3] Susan Athey and Guido W. Imbens. Identification and inference in nonlinear difference-in-differences models. *Econometrica*, 74:431–497, 2006.
- [4] Richard E. Barlow. *Statistical inference under order restrictions : the theory and application of isotonic regression*. Wiley, 1972.
- [5] Alexandre Belloni, Victor Chernozhukov, Ivan Fernandez-Val, and Christian Hansen. Program evaluation and causal inference with high-dimensional data. *Econometrica*, 85(1):233–298, 2017.
- [6] Richard Berk, Emil Pitkin, Lawrence Brown, Andreas Buja, Edward George, and Linda Zhao. Covariance adjustments for the analysis of randomized field experiments. *Evaluation review*, 37:170–196, 2013.
- [7] Undral Byambadalai, Tomu Hirata, Tatsushi Oka, and Shota Yasui. On efficient estimation of distributional treatment effects under covariate-adaptive randomization. *arXiv preprint arXiv:2506.05945*, 2025.
- [8] Undral Byambadalai, Tatsushi Oka, and Shota Yasui. Estimating distributional treatment effects in randomized experiments: Machine learning for variance reduction. 2024.
- [9] Brantly Callaway and Tong Li. Quantile treatment effects in difference in differences models with panel data. *Quantitative economics*, 10:1579–1618, 2019.
- [10] Brantly Callaway, Tong Li, and Tatsushi Oka. Quantile treatment effects in difference in differences models under dependence restrictions and with only two time periods. *Journal of Econometrics*, 206(2):395–413, 2018.
- [11] Rich Caruana. Multitask learning. *Machine Learning*, 28(1):41–75, 1997.
- [12] Victor Chernozhukov, Denis Chetverikov, Mert Demirer, Esther Duflo, Christian Hansen, Whitney Newey, and James Robins. Double/debiased machine learning for treatment and structural parameters. *The Econometrics Journal*, 21(1):C1–C68, 01 2018.
- [13] Victor Chernozhukov, Juan Carlos Escanciano, Hidehiko Ichimura, Whitney K Newey, and James M Robins. Locally robust semiparametric estimation. *Econometrica*, 90(4):1501–1535, 2022.
- [14] Victor Chernozhukov, Iván Fernández-Val, and Blaise Melly. Inference on counterfactual distributions. *Econometrica*, 81(6):2205–2268, 2013.
- [15] Victor Chernozhukov, Iván Fernández-Val, and Blaise Melly. Inference on counterfactual distributions. *Econometrica*, 81:2205–2268, 2013.
- [16] Victor Chernozhukov, Iván Fernández-Val, Blaise Melly, and Kaspar Wüthrich. Generic inference on quantile and quantile effect functions for discrete outcomes. *Journal of the American Statistical Association*, 115:123–137, 2020.

- [17] Victor Chernozhukov and Christian Hansen. An iv model of quantile treatment effects. *Econometrica*, 73:245–261, 2005.
- [18] Denis Chetverikov, Andres Santos, and Azeem M Shaikh. The econometrics of shape restrictions. *Annual review of economics*, 10:31–63, 2018.
- [19] Hugh A. Chipman, Edward I. George, and Robert E. McCulloch. Bart: Bayesian additive regression trees. *The Annals of Applied Statistics*, 4(1), March 2010.
- [20] Andrew Cotter, Maya Gupta, Heinrich Jiang, Erez Louidor, James Muller, Tamann Narayan, Serena Wang, and Tao Zhu. Shape constraints for set functions. In *International conference on machine learning*, pages 1388–1396. PMLR, 2019.
- [21] Michael Crawshaw. Multi-task learning with deep neural networks: A survey. *CoRR*, abs/2009.09796, 2020.
- [22] Krzysztof Dembczyński, Willem Waegeman, Weiwei Cheng, and Eyke Hüllermeier. On label dependence and loss minimization in multi-label classification. *Machine Learning*, 88:5–45, 2012.
- [23] Alex Deng, Ya Xu, Ron Kohavi, and Toby Walker. Improving the sensitivity of online controlled experiments by utilizing pre-experiment data. In *Proceedings of the Sixth ACM International Conference on Web Search and Data Mining*, pages 123–132. Association for Computing Machinery, 2013.
- [24] Lutz Dümbgen. Shape-constrained statistical inference. *Annual review of statistics and its application*, 11:373–391, 2024.
- [25] Paul J. Ferraro and Michael K. Price. Using nonpecuniary strategies to influence behavior: Evidence from a large-scale field experiment. *The review of economics and statistics*, 95:64–73, 2013.
- [26] Sergio Firpo. Efficient semiparametric estimation of quantile treatment effects. *Econometrica*, 75(1):259–276, 2007.
- [27] Ronald Aylmer Fisher. *The design of experiments*. Oliver and Boyd, 2nd ed. edition, 1937.
- [28] Nicole Fortin, Thomas Lemieux, and Sergio Firpo. Decomposition methods in economics. 4:1–102, 2011.
- [29] David A. Freedman. Statistical models for causation: What inferential leverage do they provide? *Evaluation review*, 30:691–713, 2006.
- [30] Markus Frölich and Blaise Melly. Unconditional quantile treatment effects under endogeneity. *Journal of Business & Economic Statistics*, 31(3):346–357, 2013.
- [31] Maya Gupta, Dara Bahri, Andrew Cotter, and Kevin Canini. Diminishing returns shape constraints for interpretability and regularization. *Advances in neural information processing systems*, 31, 2018.
- [32] Maya Gupta, Andrew Cotter, Jan Pfeifer, Konstantin Voevodski, Kevin Canini, Alexander Mangylov, Wojciech Moczydlowski, and Alexander Van Esbroeck. Monotonic calibrated interpolated look-up tables. *Journal of Machine Learning Research*, 17(109):1–47, 2016.
- [33] Trevor. Hastie. *Generalized additive models*. Chapman and Hall, 1st ed edition, 1990.
- [34] Joel L. Horowitz and Sokbae Lee. Nonparametric estimation and inference under shape restrictions. *Journal of econometrics*, 201:108–126, 2017.

- [35] Ehsan Imani and Martha White. Improving regression performance with distributional losses. 2018.
- [36] Guido W. Imbens and Donald B. Rubin. *Causal Inference for Statistics, Social, and Biomedical Sciences*. Cambridge University Press, 2015.
- [37] Liang Jiang, Peter CB Phillips, Yubo Tao, and Yichong Zhang. Regression-adjusted estimation of quantile treatment effects under covariate-adaptive randomizations. *Journal of Econometrics*, 234(2):758–776, 2023.
- [38] Nathan Kallus, Xiaojie Mao, and Masatoshi Uehara. Localized debiased machine learning: Efficient inference on quantile treatment effects and beyond. *Journal of Machine Learning Research*, 25(16):1–59, 2024.
- [39] Ron Kohavi. *Trustworthy online controlled experiments : a practical guide to A/B testing*. Cambridge University Press, 2020.
- [40] Rui Song Lan Wang, Yu Zhou and Ben Sherwood. Quantile-optimal treatment regimes. *Journal of the American Statistical Association*, 113(523):1243–1254, 2018. PMID: 30416233.
- [41] Randall A Lewis and Justin M Rao. The unfavorable economics of measuring the returns to advertising. *The Quarterly Journal of Economics*, 130(4):1941–1973, 2015.
- [42] Rui Li, Howard D. Bondell, and Brian J. Reich. Deep distribution regression, 2019.
- [43] Winston Lin. Agnostic notes on regression adjustments to experimental data: Reexamining freedman’s critique. *The annals of applied statistics*, 7:295–318, 2013.
- [44] John A. List, Ian Muir, and Gregory Sun. Using machine learning for efficient flexible regression adjustment in economic experiments. *Econometric reviews*, pages 1–39, 2024.
- [45] Rosa L. Matzkin. *Chapter 42 Restrictions of economic theory in nonparametric methods*, volume 4, pages 2523–2558. Elsevier B.V, 1994.
- [46] Tatsushi Oka, Shota Yasui, Yuta Hayakawa, and Undral Byambadalai. Regression adjustment for estimating distributional treatment effects in randomized controlled trials. 2024.
- [47] Adam Paszke, Sam Gross, Francisco Massa, Adam Lerer, James Bradbury, Gregory Chanan, Trevor Killeen, Zeming Lin, Natalia Gimelshein, Luca Antiga, Alban Desmaison, Andreas Köpf, Edward Yang, Zach DeVito, Martin Raison, Alykhan Tejani, Sasank Chilamkurthy, Benoit Steiner, Lu Fang, Junjie Bai, and Soumith Chintala. Pytorch: An imperative style, high-performance deep learning library, 2019.
- [48] Paul R. Rosenbaum. Covariance adjustment in randomized experiments and observational studies. *Statistical science*, 17:286–304, 2002.
- [49] Michael Rosenblum and Mark J van der Laan. Simple, efficient estimators of treatment effects in randomized trials using generalized linear models to leverage baseline variables. *The International Journal of Biostatistics*, 6:13–Article 13, 2010.
- [50] Christoph Rothe. Nonparametric estimation of distributional policy effects. *Journal of Econometrics*, 155(1):56–70, 2010.
- [51] Donald B Rubin. Estimating causal effects of treatments in randomized and nonrandomized studies. *Journal of educational psychology*, 66:688–701, 1974.

- [52] Donald B Rubin. Randomization analysis of experimental data: The fisher randomization test comment, 1980.
- [53] Sebastian Ruder. An overview of multi-task learning in deep neural networks. arXiv preprint arXiv:1706.05098, 2017.
- [54] Jianlin Su, Mingren Zhu, Ahmed Murtadha, Shengfeng Pan, Bo Wen, and Yunfeng Liu. Zlpr: A novel loss for multi-label classification, 2022.
- [55] Nadezhda Tagasovska and David Lopez-Paz. Single-model uncertainties for deep learning. In *Advances in Neural Information Processing Systems* 32, pages 6417–6428, 2019.
- [56] Diane Tang, Ashish Agarwal, Deirdre O’Brien, and Mike Meyer. Overlapping experiment infrastructure: More, better, faster experimentation. In *Proceedings of the 16th ACM SIGKDD international conference on Knowledge discovery and data mining*, pages 17–26, 2010.
- [57] Adane Nega Tarekegn, Mohib Ullah, and Faouzi Alaya Cheikh. Deep learning for multi-label learning: A comprehensive survey, 2024.
- [58] Anastasios A. Tsiatis, Marie Davidian, Min Zhang, and Xiaomin Lu. Covariate adjustment for two-sample treatment comparisons in randomized clinical trials: A principled yet flexible approach. *Statistics in medicine*, 27:4658–4677, 2008.
- [59] Halbert White. Nonparametric estimation of conditional quantiles using neural networks. In *Computing Science and Statistics: Statistics of Many Parameters: Curves, Images, Spatial Models*, pages 190–199. Springer, 1992.
- [60] Guojun Wu, Ge Song, Xiaoxiang Lv, Shikai Luo, Chengchun Shi, and Hongtu Zhu. Dnet: Distributional network for distributional individualized treatment effects. In *Proceedings of the 29th ACM SIGKDD Conference on Knowledge Discovery and Data Mining*, KDD ’23, page 5215–5224, New York, NY, USA, 2023. Association for Computing Machinery.
- [61] Huizhi Xie and Juliette Aurisset. Improving the sensitivity of online controlled experiments: Case studies at netflix. In *Proceedings of the 22nd ACM SIGKDD International Conference on Knowledge Discovery and Data Mining*, pages 645–654, 2016.
- [62] Huizhi Xie and Juliette Aurisset. Improving the sensitivity of online controlled experiments: Case studies at netflix. In *Proceedings of the 22nd ACM SIGKDD International Conference on Knowledge Discovery and Data Mining*, pages 645–654. ACM, 2016.
- [63] Dandan Xu, Michael J. Daniels, and Almut G. Winterstein. A bayesian nonparametric approach to causal inference on quantiles. *Biometrics*, 74(3):986–996, 2018.
- [64] Li Yang and Anastasios A Tsiatis. Efficiency study of estimators for a treatment effect in a pretest-posttest trial. *The American statistician*, 55:314–321, 2001.
- [65] Seungil You, David Ding, Kevin Canini, Jan Pfeifer, and Maya Gupta. Deep lattice networks and partial monotonic functions. In I Guyon, U Von Luxburg, S Bengio, H Wallach, R Fergus, S Vishwanathan, and R Garnett, editors, *Advances in Neural Information Processing Systems*, volume 30. Curran Associates, Inc., 2017.
- [66] Min-Ling Zhang and Zhi-Hua Zhou. Multilabel neural networks with applications to functional genomics and text categorization. *IEEE Transactions on Knowledge and Data Engineering*, 18(10):1338–1351, 2006.

- [67] Min-Ling Zhang and Zhi-Hua Zhou. A review on multi-label learning algorithms. *IEEE Transactions on Knowledge and Data Engineering*, 26(8):1819–1837, 2014.
- [68] Yu Zhang and Qiang Yang. An overview of multi-task learning. *National Science Review*, 5(1):30–43, 2018.
- [69] Yu Zhang and Qiang Yang. A survey on multi-task learning. *IEEE Transactions on Knowledge and Data Engineering*, 34(12):5586–5609, 2021.

Appendix

The Appendix is structured as follows. Appendix A summarizes the notations used in the main text and the Appendix. Appendix B provides the proofs of the theorems. Appendix C outlines the multiplier bootstrap procedure used for obtaining the confidence intervals in this paper. Appendix D describes the simulation settings, Appendix E presents the additional details of the field experiment to reduce water consumption, and Appendix F offers the supplemental information about the content promotion experiment on ABEMA.

A Summary of Notation

The notations used in the main text are summarized in Table A1.

Notation	Definition
X_i	pre-treatment covariates
W_i	treatment variable
Y_i	outcome variable
Z_i	observed samples, $Z_i := (X_i, W_i, Y_i)$
$Y_i(w)$	potential outcome for treatment group w
$\tilde{\mathcal{Y}}$	a set of scalar-valued locations to estimate the treatment effect for
π_w	treatment assignment probability for treatment group w
n_w	number of observations in treatment group w
n	number of observations
$\hat{\pi}_w$	n_w/n , estimated treatment assignment probability for treatment group w
$F_{Y^{(w)}}(y)$	$E[\mathbf{1}_{\{Y^{(w)} \leq y\}}]$, potential outcome distribution function
$\gamma_y^{(w)}(x)$	$E[\mathbf{1}_{\{Y^{(w)} \leq y\}} X = x]$, conditional distribution function
$\hat{\gamma}_y^{(w)}(x)$	estimator of conditional distribution function $\gamma_y^{(w)}(x)$
$\mathbf{\Gamma}^{(w)}$	a set of conditional distribution functions $\gamma_y^{(w)}(\cdot)$ for $y \in \tilde{\mathcal{Y}}$
$\hat{\mathbf{\Gamma}}^{(w)}$	estimator of $\mathbf{\Gamma}^{(w)}$

Table A1: Summary of Notation

B Proofs

Proof of Theorem 1

We follow the approach used in [8] to prove the efficiency gain of the adjusted estimation. For completeness of the proof, we first present a variant of Lagrange's identity and Bergström's inequality in the below lemma, which is useful to prove the efficiency gain of the regression adjustment.

Lemma 2. For any $(a_1, \dots, a_K) \in \mathbb{R}^K$ and $(b_1, \dots, b_K) \in \mathbb{R}^K$ with $b_k > 0$ for all $k = 1, \dots, K$, we can show that

$$\sum_{k=1}^K \frac{a_k^2}{b_k} - \frac{(\sum_{k=1}^K a_k)^2}{\sum_{k=1}^K b_k} = \frac{1}{\sum_{k=1}^K b_k} \cdot \frac{1}{2} \sum_{k=1}^K \sum_{\substack{\ell=1 \\ \ell \neq k}}^K \frac{(a_k b_\ell - a_\ell b_k)^2}{b_k b_\ell},$$

which implies Bergström's inequality, given by

$$\sum_{k=1}^K \frac{a_k^2}{b_k} \geq \frac{(\sum_{k=1}^K a_k)^2}{\sum_{k=1}^K b_k}.$$

Proof. Lagrange's identity is that, for any $(c_1, \dots, c_K) \in \mathbb{R}^K$ and $(d_1, \dots, d_K) \in \mathbb{R}^K$,

$$\left(\sum_{k=1}^K c_k^2 \right) \left(\sum_{k=1}^K d_k^2 \right) - \left(\sum_{k=1}^K c_k d_k \right)^2 = \frac{1}{2} \sum_{k=1}^K \sum_{\substack{\ell=1 \\ \ell \neq k}}^K (c_k d_\ell - c_\ell d_k)^2. \quad (4)$$

Fix arbitrary $(a_1, \dots, a_K) \in \mathbb{R}^K$ and $(b_1, \dots, b_K) \in \mathbb{R}^K$ with $b_k > 0$ for all $k = 1, \dots, K$. Then, taking $c_k = a_k / \sqrt{b_k}$ and $d_k = \sqrt{b_k}$ for all $k = 1, \dots, K$ in (4), we can show that

$$\begin{aligned} \left(\sum_{k=1}^K \frac{a_k^2}{b_k} \right) \left(\sum_{k=1}^K b_k \right) - \left(\sum_{k=1}^K a_k \right)^2 &= \frac{1}{2} \sum_{k=1}^K \sum_{\substack{\ell=1 \\ \ell \neq k}}^K \left(\frac{a_k}{\sqrt{b_k}} \sqrt{b_\ell} - \frac{a_\ell}{\sqrt{b_\ell}} \sqrt{b_k} \right)^2 \\ &= \frac{1}{2} \sum_{k=1}^K \sum_{\substack{\ell=1 \\ \ell \neq k}}^K \frac{(a_k b_\ell - a_\ell b_k)^2}{b_k b_\ell}, \end{aligned}$$

which leads to the desired equality. Also, the last expression in the math display above is non-negative, which leads to Bergström's inequality. \square

To establish Theorem 1, we first introduce additional notation. Specifically, we define the empirical probability measures of X as

$$\widehat{\mathbb{F}}_X := \frac{1}{n} \sum_{i=1}^n \delta_{X_i} \quad \text{and} \quad \widehat{\mathbb{F}}_X^{(w)} := \frac{1}{n_w} \sum_{i=1}^n \mathbf{1}_{\{W_i=w\}} \cdot \delta_{X_i},$$

for all observations and observations in the treatment group $w \in \mathcal{W}$, respectively. Here, δ_x is the measure that assigns mass 1 at $x \in \mathcal{X}$ and thus $\widehat{\mathbb{F}}_X$ and $\widehat{\mathbb{F}}_X^{(w)}$ can be interpreted as the random discrete probability measures, which put mass $1/n$ and $1/n_w$ at each of the n and n_w points $\{X_i\}_{i=1}^n$ and $\{X_i : W_i = w\}_{i=1}^n$, respectively. Given a real-valued function $f : \mathcal{X} \rightarrow \mathbb{R}$, we denote by

$$\widehat{\mathbb{F}}_X f = \int f d\widehat{\mathbb{F}}_X = \frac{1}{n} \sum_{i=1}^n f(X_i)$$

and

$$\widehat{\mathbb{F}}_X^{(w)} f = \int f d\widehat{\mathbb{F}}_X^{(w)} = \frac{1}{n_w} \sum_{i=1}^n \mathbf{1}_{\{W_i=w\}} \cdot f(X_i).$$

Given that the true conditional distribution $\gamma_y^{(w)}(X) \equiv F_{Y(w)|X}(y|X)$, the infeasible version of regression-adjusted distribution function for treatment $w \in \mathcal{W}$ is written as

$$\widetilde{\mathbf{F}}_{Y(w)}(y) = \widehat{\mathbf{F}}_{Y(w)}^{\text{empirical}}(y) - (\widehat{\mathbb{F}}_X^{(w)} - \widehat{\mathbb{F}}_X) \gamma_y^{(w)}.$$

Proof of Theorem 1. Part (a) Choose any arbitrary $w \in \mathcal{W}$ and $y \in \mathcal{Y}$. Applying the quadratic expansion for $\tilde{\mathbf{F}}_{Y(w)}(y) = \hat{\mathbf{F}}_{Y(w)}^{\text{empirical}}(y) - (\hat{\mathbb{F}}_X^{(w)} - \hat{\mathbb{F}}_X)\gamma_y^{(w)}$, we can show that

$$\text{Var}(\tilde{\mathbf{F}}_{Y(w)}(y)) = \text{Var}(\hat{\mathbf{F}}_{Y(w)}^{\text{empirical}}(y)) - 2\text{Cov}\left(\hat{\mathbf{F}}_{Y(w)}^{\text{empirical}}(y), (\hat{\mathbb{F}}_X^{(w)} - \hat{\mathbb{F}}_X)\gamma_y^{(w)}\right) + \text{Var}\left((\hat{\mathbb{F}}_X^{(w)} - \hat{\mathbb{F}}_X)\gamma_y^{(w)}\right). \quad (5)$$

We can write $\hat{\mathbb{F}}_X = \sum_{w' \in \mathcal{W}} \hat{\pi}_{w'} \hat{\mathbb{F}}_X^{(w')}$. It is assumed that observations are a random sample and $n_{w'}/n = \pi_{w'} + o(1)$ for every $w' \in \mathcal{W}$ as $n \rightarrow \infty$. Furthermore, all unconditional and conditional functions are bounded. By applying the dominated convergence theorem, we can show

$$\begin{aligned} n\text{Cov}\left(\hat{\mathbf{F}}_{Y(w)}^{\text{empirical}}(y), (\hat{\mathbb{F}}_X^{(w)} - \hat{\mathbb{F}}_X)\gamma_y^{(w)}\right) &= n\text{Cov}\left(\hat{\mathbf{F}}_{Y(w)}^{\text{empirical}}(y), (1 - \hat{\pi}_w)\hat{\mathbb{F}}_X^{(w)}\gamma_y^{(w)}(X)\right) \\ &= \frac{1 - \pi_w}{\pi_w} \text{Cov}(\mathbf{1}_{\{Y(w) \leq y\}}, \gamma_y^{(w)}(X)) + o(1). \end{aligned} \quad (6)$$

Similarly, we can show that

$$\begin{aligned} n\text{Var}\left((\hat{\mathbb{F}}_X^{(w)} - \hat{\mathbb{F}}_X)\gamma_y^{(w)}\right) &= n\text{Var}\left((1 - \hat{\pi}_w)\hat{\mathbb{F}}_X^{(w)}\gamma_y^{(w)}\right) + n \sum_{w': w' \neq w} \text{Var}\left(\hat{\pi}_{w'}\hat{\mathbb{F}}_X^{(w')}\gamma_y^{(w')}\right) \\ &= \frac{(1 - \pi_w)^2}{\pi_w} \text{Var}(\gamma_y^{(w)}(X)) + \sum_{w': w' \neq w} \frac{\pi_{w'}^2}{\pi_{w'}} \text{Var}(\gamma_y^{(w')}(X)) + o(1) \\ &= \left(\frac{(1 - \pi_w)^2}{\pi_w} + \sum_{w': w' \neq w} \pi_{w'}\right) \text{Var}(\gamma_y^{(w)}(X)) + o(1) \\ &= \frac{1 - \pi_w}{\pi_w} \text{Var}(\gamma_y^{(w)}(X)) + o(1). \end{aligned} \quad (7)$$

It follows from (5)-(7) that

$$n\left\{\text{Var}(\hat{\mathbf{F}}_{Y(w)}^{\text{empirical}}(y)) - \text{Var}(\tilde{\mathbf{F}}_{Y(w)}(y))\right\} = \frac{1 - \pi_w}{\pi_w} \left\{2\text{Cov}(\mathbf{1}_{\{Y(w) \leq y\}}, \gamma_y^{(w)}(X)) - \text{Var}(\gamma_y^{(w)}(X))\right\} + o(1). \quad (8)$$

An application of the law of iterated expectation yields

$$\text{Cov}(\mathbf{1}_{\{Y(w) \leq y\}}, \gamma_y^{(w)}(X)) = \text{Var}(E[\mathbf{1}_{\{Y(w) \leq y\}}|X]),$$

which together with (8) shows

$$n\left\{\text{Var}(\hat{\mathbf{F}}_{Y(w)}^{\text{empirical}}(y)) - \text{Var}(\tilde{\mathbf{F}}_{Y(w)}(y))\right\} = \frac{1 - \pi_w}{\pi_w} \text{Var}(\gamma_y^{(w)}(X)) + o(1).$$

Since $\pi_w \in (0, 1)$ and $\text{Var}(\gamma_y^{(w)}(X)) \geq 0$, it follows that $\text{Var}(\hat{\mathbf{F}}_{Y(w)}^{\text{empirical}}(y)) \geq \text{Var}(\tilde{\mathbf{F}}_{Y(w)}(y)) + o(n^{-1})$. Here, the equality hold only when $F_{Y(w)|X}(y) = F_{Y(w)}(y)$ or X has no predictive power for the event $\mathbf{1}_{\{Y(w) \leq y\}}$.

Part (b) Choose any arbitrary $y \in \mathcal{Y}$. First, we shall show that, for any $w, w' \in \mathcal{W}$,

$$n\text{Cov}(\hat{\mathbf{F}}_{Y(w)}(y), \tilde{\mathbf{F}}_{Y(w')}(y)) = \text{Cov}(\gamma_y^{(w)}(X), \gamma_y^{(w')}(X)). \quad (9)$$

Fix any two distinct treatment statuses $w, w' \in \mathcal{W}$. We can write $\tilde{\mathbf{F}}_{Y(w)}(y) = (\hat{\mathbf{F}}_{Y(w)}^{empirical}(y) - \hat{\mathbb{F}}_X^{(w)} \gamma_y^{(w)}) + \hat{\mathbb{F}}_X \gamma_y^{(w)}$ and also $\hat{\mathbb{F}}_X \gamma_y^{(w)} = \sum_{v \in \mathcal{W}} \hat{\pi}_v \hat{\mathbb{F}}_X^{(v)} \gamma_y^{(w)}$. Given random sample and the bi-linear property of the covariance function, we can show that

$$\begin{aligned} \text{Cov}\left(\tilde{\mathbf{F}}_{Y(w)}(y), \tilde{\mathbf{F}}_{Y(w')}(y)\right) &= \text{Cov}\left(\hat{\mathbf{F}}_{Y(w)}^{empirical}(y) - \hat{\mathbb{F}}_X^{(w)} \gamma_y^{(w)}, \hat{\pi}_{w'} \hat{\mathbb{F}}_X^{(w')} \gamma_y^{(w')}\right) \\ &\quad + \text{Cov}\left(\hat{\pi}_w \hat{\mathbb{F}}_X^{(w)} \gamma_y^{(w)}, \hat{\mathbf{F}}_{Y(w')}^{empirical} - \hat{\mathbb{F}}_X^{(w')} \gamma_y^{(w')}\right) \\ &\quad + \text{Cov}\left(\hat{\mathbb{F}}_X \gamma_y^{(w)}, \hat{\mathbb{F}}_X \gamma_y^{(w')}\right), \end{aligned}$$

where it can be shown that the first and second terms on the right-hand side are equal zero, due to the fact that $E\left[\hat{\mathbf{F}}_{Y(w)}^{empirical}(y) - \hat{\mathbb{F}}_X^{(w)} \gamma_y^{(w)} \mid X_1, \dots, X_n\right] = 0$. Furthermore, under the random sample assumption, we can show that

$$\text{Cov}\left(\hat{\mathbb{F}}_X \gamma_y^{(w)}, \hat{\mathbb{F}}_X \gamma_y^{(w')}\right) = n^{-1} \text{Cov}\left(\gamma_y^{(w)}(X), \gamma_y^{(w')}(X)\right)$$

. Thus, we can prove the equality in (9).

Next, we compare the variance-covariance matrices of the simple and regression-adjusted estimators. By applying the result from part (a) of this theorem and the one in (9), we are able to show that

$$\begin{aligned} n\{\text{Var}(\hat{\theta}_y^{empirical}) - \text{Var}(\tilde{\theta}_y)\} &= \begin{bmatrix} \frac{1-\pi_1}{\pi_1} \text{Var}(\gamma_y^{(1)}(X)), & -\text{Cov}(\gamma_y^{(1)}(X), \gamma_y^{(2)}(X)), & \dots, & -\text{Cov}(\gamma_y^{(1)}(X), \gamma_y^{(K)}(X)) \\ -\text{Cov}(\gamma_y^{(2)}(X), \gamma_y^{(1)}(X)), & \frac{1-\pi_2}{\pi_2} \text{Var}(\gamma_y^{(2)}(X)), & \dots, & -\text{Cov}(F_{Y(2)|X}, F_{Y(K)|X}) \\ \vdots & \vdots & \ddots & \vdots \\ -\text{Cov}(\gamma_y^{(K)}(X), \gamma_y^{(1)}(X)), & -\text{Cov}(\gamma_y^{(K)}(X), \gamma_y^{(2)}(X)), & \dots, & \frac{1-\pi_K}{\pi_K} \text{Var}(\gamma_y^{(K)}(X)) \end{bmatrix} + o(1), \end{aligned}$$

which can be written as

$$n\{\text{Var}(\hat{\theta}_y^{empirical}) - \text{Var}(\tilde{\theta}_y)\} = E\left[(\gamma_y(X) - E[\gamma_y(X)]) A (\gamma_y(X) - E[\gamma_y(X)])^\top\right] + o(1),$$

where $\gamma_y(X) = [\gamma_y^{(1)}(X), \dots, \gamma_y^{(K)}(X)]^\top$ and

$$A := \begin{bmatrix} \pi_1^{-1} - 1, & -1, & \dots, & -1 \\ -1, & \pi_2^{-1} - 1, & \dots, & -1 \\ \vdots & \vdots & \ddots & \vdots \\ -1, & -1, & \dots, & \pi_K^{-1} - 1 \end{bmatrix}.$$

The variant of Lagrange's identity in Lemma 2 with $\sum_{w \in \mathcal{W}} \pi_w = 1$ shows that, for an arbitrary vector $v := (v_1, \dots, v_K)^\top \in \mathbb{R}^k$,

$$\begin{aligned} &v^\top (\gamma_y(X) - E[\gamma_y(X)]) A (\gamma_y(X) - E[\gamma_y(X)])^\top v \\ &= \sum_{w \in \mathcal{W}} \frac{v_w^2 (\gamma_y^{(w)}(X) - E[\gamma_y^{(w)}(X)])^2}{\pi_w} - \left(\sum_{w \in \mathcal{W}} v_w (\gamma_y^{(w)}(X) - E[\gamma_y^{(w)}(X)]) \right)^2 \\ &= \frac{1}{2} \sum_{w \in \mathcal{W}} \sum_{\substack{w' \in \mathcal{W} \\ w' \neq w}} \frac{\{v_w (\gamma_y^{(w)}(X) - E[\gamma_y^{(w)}(X)]) \pi_{w'} - v_{w'} (\gamma_y^{(w')}(X) - E[\gamma_y^{(w')}(X)]) \pi_w\}^2}{\pi_w \pi_{w'}}. \end{aligned}$$

It follows that

$$v^\top \{ \text{Var}(\widehat{\theta}_y^{\text{empirical}}) - \text{Var}(\widetilde{\theta}_y) \} v = \frac{1}{2} \sum_{w \in \mathcal{W}} \sum_{\substack{w' \in \mathcal{W} \\ w' \neq w}} \frac{\text{Var}(v_w \gamma_y^{(w)}(X) \pi_{w'} - v_{w'} \gamma_y^{(w')}(X) \pi_w)}{\pi_w \pi_{w'}} + o(n^{-1}).$$

The above equality implies the desired positive semi-definiteness result, because $\text{Var}(v_w \gamma_y^{(w)}(X) \pi_{w'} - v_{w'} \gamma_y^{(w')}(X) \pi_w) \geq 0$ for any $w, w' \in \mathcal{W}$ with $w \neq w'$.

Furthermore, the positive definite result holds when $\text{Var}(v_w \gamma_y^{(w)}(X) \pi_{w'} - v_{w'} \gamma_y^{(w')}(X) \pi_w) > 0$ for any $v \in \mathbb{R}^k$ with $v \neq 0$ and for any $w, w' \in \mathcal{W}$ with $w \neq w'$. Because $v \in \mathbb{R}^k$ is chosen arbitrarily except $v \neq 0$ and $\pi_w \in (0, 1)$ for all $w \in \mathcal{W}$, the condition for the positive definiteness can be written as $\text{Var}(\gamma_y^{(w)}(X) - r \cdot \gamma_y^{(w')}(X)) > 0$ for any $r \in \mathbb{R}$ and for any $w, w' \in \mathcal{W}$ with $w \neq w'$. \square

C Multiplier Bootstrap Procedure

We obtain pointwise confidence bands for distributional parameters, which are functionals of distribution functions, using multiplier bootstrap following [14] and [5]. We outline the procedure to obtain pointwise confidence bands in Algorithm 3 where $\phi((\theta_y)_{y \in \mathcal{Y}})$ is some functional of $(\theta_y)_{y \in \mathcal{Y}}$.

As a prerequisite, letting $\pi := (\pi_1, \dots, \pi_K)^\top$, define moment functions

$$\psi_y(Z; \theta_y, \gamma_y, \pi) := (\psi_y^{(1)}(Z; \theta_y, \gamma_y, \pi_1), \dots, \psi_y^{(K)}(Z; \theta_y, \gamma_y, \pi_K))^\top,$$

where, for each $w \in \mathcal{W}$,

$$\psi_y^{(w)}(Z; \theta_y, \gamma_y, \pi_w) := \frac{\mathbf{1}_{\{W=w\}} \cdot (\mathbf{1}_{\{Y \leq y\}} - \gamma_y^{(w)}(X))}{\pi_w} + \gamma_y^{(w)}(X) - \theta_y^{(w)}. \quad (10)$$

Algorithm 3 Multiplier bootstrap procedure to obtain pointwise confidence bands

Input: Data $\{(X_i, W_i, Y_i)\}_{i=1}^n$; point estimates $\hat{\theta}_y$; influence functions $\hat{\psi}_y(Z_i) := \psi_y(Z_i; \hat{\theta}_y, \hat{\gamma}_y, \hat{\pi})$

- (1) Draw multipliers $\{\xi_i\}_{i=1}^n = \{m_{1,i}/\sqrt{2} + ((m_{2,i})^2 - 1)/2\}_{i=1}^n$ independently from the data $\{Z_i\}_{i=1}^n$, where $m_{1,i}$ and $m_{2,i}$ are i.i.d. draws from two independent standard normal random variables.
- (2) For each $y \in \mathcal{Y}$, obtain the bootstrap draws $\phi^b(\hat{\theta}_y)$ of $\phi(\hat{\theta}_y)$ as

$$\phi^b(\hat{\theta}_y) = \phi(\hat{\theta}_y^b) \text{ where } \hat{\theta}_y^b = \hat{\theta}_y + \frac{1}{n} \sum_{i=1}^n \xi_i \hat{\psi}_y(Z_i).$$

- (3) Repeat (1)-(2) B times and index the bootstrap draws by $b = 1, \dots, B$.
- (4) Obtain bootstrap standard error estimates for $\phi(\hat{\theta}_y)$ for each $y \in \mathcal{Y}$ as

$$\hat{\Sigma}(y) = \sum_{b=1}^B \frac{(\phi^b(\hat{\theta}_y) - \bar{\phi}(\hat{\theta}_y))^2}{B-1},$$

where $\bar{\phi}(\hat{\theta}_y) = \sum_{b=1}^B \frac{\phi^b(\hat{\theta}_y)}{B}$.

- (5) Construct $(1 - \alpha) \times 100\%$ pointwise confidence band for $\phi((\theta_y)_{y \in \mathcal{Y}})$ as

$$I^{1-\alpha} := \{[\phi(\hat{\theta}_y) \pm \hat{z}_{1-\alpha} \times \hat{\Sigma}(y)] : y \in \mathcal{Y}\}.$$

Result: $(1 - \alpha) \times 100\%$ confidence band $I^{1-\alpha}$ for $\phi((\theta_y)_{y \in \mathcal{Y}})$

D Simulation Study

Here, we describe the parameters used in the simulation experiment and present additional experimental results not included in the main text. The first subsection describes the data generating process, the second subsection states the parameter details of the ML models and experiment environment, and the third subsection shows the numerical results of the simulation experiment.

D.1 Data Generating Process (DGP)

For the simulation experiment, we used the following DGP. We fix the number of covariates d_x as $d_x = 20$ and the sample size n to be $n = 1000$. For each $i = 1, \dots, n$, we generate $X_i = (X_{1i}, \dots, X_{20i})$ from $U_{20}((0, 1)^{20})$, a multivariate uniform distribution on $(0, 1)$. Binary treatment variable W_i follows a Bernoulli distribution with a success probability of $\rho = 0.5$. A continuous outcome variable Y_i is then generated from the outcome equation $Y_i = f(X_i, W_i) + U_i$, where the error term $U_i \sim N(0, 1)$. We consider the functional form of

$$f(X_i, W_i) = \sum_{j=1}^{20} \sum_{k=1}^{20} \beta_j \beta_k X_{ji} X_{ki} \tag{11}$$

so that the outcome includes the interactions of covariates. For coefficients β_j , we set

$$\beta_j = \begin{cases} 1 & \text{for } j \in \{1, \dots, 18\} \\ W_i & \text{for } j \in \{19, 20\} \end{cases}$$

Because β_{19} and β_{20} depend on the treatment variable, the records with $W_i = 1$ are more likely to take higher outcome values. We used quantiles $q \in \{0.05, 0.1, \dots, 0.95\}$ for the locations, and observed a negative DTE across all of them. The absolute size of the DTE takes the maximum around the median of the outcome distribution.

D.2 Model Implementation and Experiment Environment

The model used for the simulation study follows the structure in Figure 2 with the following parameters in Table A2. Here, h_i denotes the number of neurons in the i th hidden layer, Optimizer is the optimization algorithm for training neural networks, and Folds L is the number of folds used for cross-fitting. The models are trained with binary cross-entry loss and Adam Optimizer. We implemented the experiment in Python and used the PyTorch [47] framework to build the models. Experiments are run on a Macbook Pro with 36 GB memory and the Apple M3 Pro chip. The multi-task regression adjustment algorithm is available in the Python library `dte-adj` (<https://pypi.org/project/dte-adj/>). All models are trained on the CPU, and the same environment was used for all experiments.

Parameter	Simulation	Water Consumption	ABEMA
Input size d_x	20	12	10
Number of hidden layers	3	3	3
h_1	128	128	16
h_2	64	64	16
h_3	19	200	51
g	<i>exp</i>	<i>exp</i>	<i>exp</i>
$f(x)$	$\arctan(x)/(\pi/2)$	$\frac{1-\exp(-x)}{1+\exp(-x)}$	$\arctan(x)/(\pi/2)$
σ	ReLU	ReLU	ReLU
Learning Rate	0.01	0.001	0.001
Batch Size	16	64	128
Folds L	2	2	2

Table A2: Model Parameters for Empirical Studies
Notes: All neural network models use identical parameters, including the number of folds and batch size except for the size of the last hidden layer.

D.3 Pointwise Estimation Result

The pointwise MSE reduction (%) is summarized in Table A3 and its raw values per location are available in Table A4. In Table A3, the minimum, 25 percentile, median, 75 percentile and the maximum of pointwise SE reduction are reported. As shown in the result, the multi-task NN with the monotonic constraint achieves the highest MSE reduction in most locations, while the multi-task NN also outperforms the other two methods. We also applied BART [19], Wu et al. [60], and DNet [37] to our DGP and compared our DTE MSE reduction (%) with their QTE MSE reduction (%) as reported below. BART and DNet are not designed to estimate unconditional QTE precisely, while Jiang et al. proposed a regression-adjustment method like ours, designed to decrease the variance of QTE estimations compared to unadjusted QTE. The result shows that

the proposed multi-task NN adjustment achieves a higher variance reduction than BART and Jiang et al. and improves the variance across all quantiles, unlike DNet.

Method	min	p25	p50	p75	max
Linear Regression	18.2	32.7	45.5	49.0	51.7
Single-Task NN	12.2	33.6	38.7	42.6	46.7
Multi-Task NN	48.6	58.3	59.7	62.3	65.5
Monotonic Multi-Task NN	50.1	60.7	62.1	64.6	67.5

Table A3: MSE Reduction in DTE Estimation: Simulation Study

Notes: Percentage reduction in mean squared errors compared to empirical DTE across models. Sample size $n=1,000$ with $S=500$ simulation iterations.

Quantile	Linear Regression (DTE)	Single-Task NN (DTE)	Multi-Task NN (DTE)	Monotonic Multi-Task NN (DTE)	DNet (QTE)	Jiang et al. (QTE)	BART (QTE)
0.05	18.20	16.45	51.38	50.05	-449.32	18.48	-35.44
0.10	27.99	32.49	57.99	58.23	-290.99	29.02	0.17
0.15	32.36	34.66	59.79	63.38	-229.61	36.59	-2.01
0.20	36.41	39.81	59.66	62.86	-143.00	37.28	11.80
0.25	38.51	39.52	60.61	60.88	-85.91	45.38	6.25
0.30	45.53	45.91	65.14	64.92	-28.17	51.06	12.83
0.35	45.65	46.40	65.52	66.27	38.71	50.54	10.69
0.40	46.54	46.66	65.27	66.87	68.05	52.97	6.42
0.45	48.10	43.06	63.08	65.97	82.56	52.71	11.06
0.50	51.72	43.97	64.48	67.48	89.63	55.91	7.48
0.55	50.73	42.05	61.61	64.36	81.49	57.83	11.81
0.60	49.91	38.69	58.28	62.20	61.27	53.70	6.03
0.65	50.53	41.65	58.86	60.99	32.96	54.96	13.17
0.70	50.70	38.59	58.63	61.97	10.43	51.11	8.94
0.75	46.45	38.25	60.60	62.88	-44.92	47.14	12.72
0.80	38.19	35.67	58.78	60.49	-80.15	45.94	5.94
0.85	33.09	27.68	58.33	60.86	-159.48	36.40	11.59
0.90	29.32	24.91	51.38	56.10	-174.35	35.02	8.00
0.95	20.71	12.23	48.64	52.64	-154.77	24.29	-2.17

Table A4: Pointwise MSE reduction (%) relative to the empirical DTE or QTE across different estimation methods in the simulation study. $n=1,000$, $S=500$.

Model	Accuracy ↑	Precision ↑	Recall ↑
Linear Regression	0.933	0.937	0.928
Single-Task NN	0.891	0.889	0.892
Multi-Task NN	0.954	0.946	0.963
Monotonic Multi-Task NN	0.959	0.970	0.945

Table A5: Comparison of prediction performance on the simulation data.

E Nudges to Reduce Water Consumption

Here, we describe the parameters used in Nudges to Reduce Water Consumption experiment and present additional experimental results that were not included in the main text. The dataset from the randomized experiment can be downloaded at <https://doi.org/10.7910/DVN1/22633> [25]. The covariates used for this experiment are monthly water consumption during the year prior to the experiment. The locations used for this experiment are $\tilde{\mathcal{Y}} = (1, \dots, 199, 200)^T$ and Figure A1 shows the histogram of outcomes. As described in the main text, most records are distributed from 0 to 100 and the range 100 to 200 contains a limited number of records. The parameters used for this experiment are described in Table A2. The numerical results in Table A6 align with the simulation experiment, showing that the multi-task neural network outperforms the other two methods, with the monotonic constraint further enhancing precision.

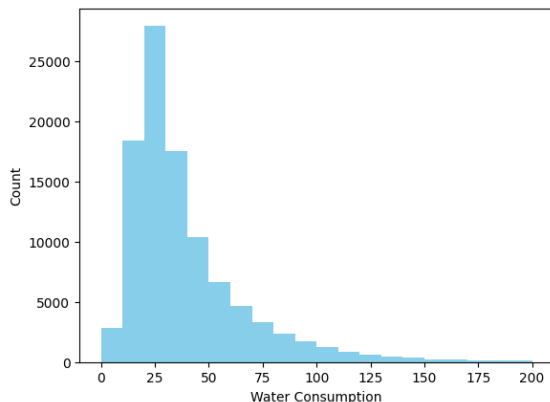


Figure A1: Water Consumption Distribution
Notes: Values in thousands of gallons. Most observations range between 0 and 100 thousand gallons.

Method	min	p25	p50	p75	max
Linear Regression	-0.35	7.39	12.6	20.5	26.5
Single-Task NN	-2.11	12.6	18.2	28.7	33.0
Multi-Task NN	6.78	17.4	19.1	29.5	32.9
Monotonic Multi-Task NN	3.08	17.5	20.3	29.5	33.3

Table A6: Summary of SE Reduction in DTE Estimation (%): Water Conservation Experiment
Notes: Percentage reduction in standard errors compared to the empirical DTE across models. Sample size $n=78,500$ with $B=5,000$ multiplier bootstrap iterations.

F ABEMA Content Promotion

Here, we describe the parameters used in the ABEMA content promotion experiment and present additional experimental results that were not included in the main text. The locations used for this experiment are $\tilde{\mathcal{Y}} = (0, 1, \dots, 50)^T$. Table A7 presents the numerical values of the MSE reduction rate. As in the previous two experiments, the multi-task NN and monotonic multi-task NN adjustments outperform the other two adjustment methods. Unlike the other two experiments, no clear improvement was seen by the monotonicity constraint. We hypothesize that the large sample size in this experiment eliminates the need for neural

network models to benefit from the monotonic constraint. The parameters used for this experiment are described in Table A2. We limit the size of neurons in the NN in this experiment due to its large sample size.

Method	min	p25	p50	p75	max
Linear Regression	0.406	5.10	6.31	7.16	14.3
Single-Task NN	0.249	5.49	6.45	7.86	15.3
Multi-Task NN	0.305	5.65	7.02	7.95	15.7
Monotonic Multi-Task NN	0.310	5.65	7.01	7.95	15.7

Table A7: Summary of SE Reduction in DTE Estimation (%): ABEMA Content Promotion
Notes: SE reduction (%) is calculated over the empirical DTE across models. Sample size $n=4,311,905$ with $B=5,000$ multiplier bootstrap iterations.

G Validity of Sub-linear Assumption

G.1 Computational Analysis of Linear Regression

Consider the following notation:

- $X \in \mathbb{R}^{n \times d}$: input matrix
- $Y \in \mathbb{R}^{n \times p}$: output matrix with p target dimensions
- $B \in \mathbb{R}^{d \times p}$: parameter matrix

We assume $n \gg d, p$.

Joint Multivariate Linear Regression. The closed-form solution for joint multivariate linear regression is given by

$$B = (X^\top X)^{-1} X^\top Y.$$

The computational complexity consists of the following components:

- $\mathcal{O}(nd^2)$ for computing $X^\top X$
- $\mathcal{O}(d^3)$ for matrix inversion
- $\mathcal{O}(ndp)$ for computing $X^\top Y$
- $\mathcal{O}(d^2p)$ for the final matrix multiplication

Therefore, the total computational cost of joint multivariate linear regression is

$$\mathcal{O}(nd^2 + d^3 + ndp + d^2p). \tag{12}$$

Separate Univariate Linear Regression. For training univariate linear regression separately, we compute the regression coefficient for each output dimension $y^{(i)} \in \mathbb{R}^n$:

$$\beta^{(i)} = (X^\top X)^{-1} X^\top y^{(i)}.$$

The computational cost per output dimension $y^{(i)}$ is $\mathcal{O}(nd^2 + d^3)$. Consequently, the total computational cost over all p outputs is

$$\mathcal{O}(pnd^2 + pd^3). \tag{13}$$

Efficiency Comparison. Given that $n \gg d, p$, we observe that

$$\mathcal{O}(nd^2 + d^3 + ndp + d^2p) \ll \mathcal{O}(pnd^2 + pd^3), \tag{14}$$

which demonstrates that linear regression satisfies the sub-linear computational scaling property outlined in Assumption 3, confirming that joint estimation provides significant computational advantages over separate univariate approaches.

G.2 Empirical Computation Complexity Analysis of Neural Networks

We hypothesize that deeper architectures, such as ResNet can achieve substantially higher computational cost reduction under our proposed framework. To empirically validate this hypothesis, we analyze the computational complexity of several neural network architectures by measuring multiply-accumulate (MAC) operations for models with single versus multiple outputs using the `ptflop` Python library.

Model	1 output	20 outputs
Our Dense NN	11.2 K	12.4 K
BERT	852.23 M	852.24 M
ResNet-18	1.82 G	1.82 G

Table A8: Computational complexity comparison across different neural network architectures measured in MAC operations

These results demonstrate that complex models satisfy the sub-linear scaling property outlined in Assumption 3. Notably, the computational complexity of both BERT and ResNet-18 remains virtually unchanged when scaling from single to multiple outputs, confirming near-constant computational overhead. This behavior arises because modern deep architectures such as convolutional neural networks (CNNs) and Transformers typically employ deep encoding layers that extract shared representations, making them particularly well-suited for our multi-task learning approach.